10th CIRP Conference on Photonic Technologies [LANE 2018]

From statistic to deterministic nanostructures in fused silica induced by nanosecond laser radiation

Pierre Lorenz[a],*, Michael Klöppel[b], Igor Zagoranskiy[a], Klaus Zimmer[a]

aLeibniz-Institut für Oberflächenmodifizierung e. V.,Permoserstr. 15, 04318 Leipzig, Germany
bFraunhofer-Institut für Verkehrs- und Infrastruktursysteme IVI, Germany

* Corresponding author. Tel.: +49-341-235-3291 ; fax: +49-341-235-2584. *E-mail address:* pierre.lorenz@iom-leipzig.de

Abstract

The production of structures by laser machining below the diffraction limit is still a challenge. However, self-organization processes can be useful. The laser-induced self-organized modification of the shape of photolithographic produced chromium structures on fused silica as well as the structuring of the fused silica surface by nanosecond UV laser radiation was studied, respectively. Low fluence single pulse laser irradiation ($\square$ > 300 mJ/cm²) cause the formation from chromium squares to droplets due to the mass transport in the molten chromium film. This process is governed by the instability of the molten metal due to the surface tension driven liquid phase mass transport. For a chromium pattern size similar to the instability length two specific droplet distributions were found which are single droplets with a determined position near the centre of the original pattern or random distributed smaller droplets arranged circularly. Each of the metal patterns can be transferred into the fused silica by a multi-pulse irradiation. The experimental results can be simulated well for low fluences by sequential solving the heat and Navier-Stokes equation.

1. Introduction

The fabrication of determined and randomly distributed sub-µm and nanostructures by laser method is challenging. The "classical" laser etching methods allow the structuring of dielectric surfaces [1-6] with vertical nanometer precision and the lateral precision is in the sub-µm range and defined by the diffraction limit. The shape of the resultant structures is dependent on the laser parameter and especially on the beam profile. The usage of periodically modulated beam profiles, e.g., induced by phase mask allows the periodic sub-micrometre structuring of dielectric surfaces [6]. The IPSM-LIFE (**L**aser-**i**nduced **f**ront side **e**tching using **i**n-situ **p**re-**s**tructured **m**etal layer) method allows the fabrication of structures in dielectric surfaces with resultant lateral structure sizes below the diffraction limit [7-10]. At the IPSM-LIFE, process a dielectric surface covered by a thin metal layer is

irradiated. The process can be separated into two steps. At step 1, the laser irradiation induces a molten metal film. The mass transport in the liquid metal is induced by surface tension and the following resolidification result in a nanostructured metal film [7-10]. Furthermore, the irradiation of sub-micrometre metal structures e.g. produced by nanosphere lithography allows the defined modification of the shape of the metal structures [11]. The laser-solid interaction as well as the liquid phase mass transport is well-known [12]. Additionally, the time-behaviour of the nanostructuring process was analyzed by optical reflection and transmission measurements and shadowgraphy [12]. At step 2, the irradiation of the nanostructured metal film or metal structure results in an evaporation of the metal and partial evaporation of the dielectric surface, where the resultant structures in the dielectric surface are dependent on the metal nanostructures as well as on the laser parameters [7-10].

2. Experimental Set-up

In this study, the laser irradiation of photolithographic produced thin chromium structures on fused silica was investigated. The fused silica substrate (thickness 370 nm, roughness 1.2 nm RMS) was covered with a thin chromium layer (6.9 ± 0.5) nm by magnetron sputtering. After that, the chromium / fused silica system was covered with photoresist (AR-N4240) by spin coating and the photoresist was structured by photolithography. Then the chromium was etched by $(NH_4)_2Ce(NO_3)_6$: $HClO_4$: H_2O and finally the residual photoresist was removed. The resultant periodical chromium structures exhibit lateral sizes from ~ 0.8 x 0.8 µm² to ~5.2 x 5.2 µm², where this study is focused on ~ 2.5 x 2.5 µm² patterns. The structured chromium on fused silica was irradiated by a KrF excimer laser with a wavelength of λ = 248 nm, a pulse duration of Δt_p = 25 ns as well as a repetition rate of f = 100 Hz. An energy deviation below 5% rms can be achieved thanks to the beam shaping and homogenization optics at an irradiation area of 100 x 100 µm². The impact of the laser fluences Φ (~320 mJ/cm² to ~2.3 J/cm²) and the number of laser pulses N (1 to 1000) to the resultant structures were studied. The laser-irradiated surfaces were imaged by scanning electron microscopy (SEM) after magnetron sputtering a ~10 nm gold layer. Furthermore, suitable resultant surface topography was measured by white light interferometry (WLI).
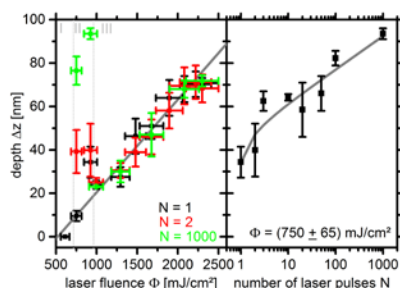
3. Results

Fig. 1. Depth in fused silica measured by WLI induced by the irradiation of Cr/SiO_2 system with different laser fluences Φ and number of laser pulses N (grey line: analytical approximation of the dependency:
(left): $\Delta z(\Phi)=m*(\Phi-\Phi_{th})$ (m = 0.004726 nm/(mJ/cm²), Φ_{th} = 521.88 mJ/cm²)
(right): $\Delta z(N) = a + b * \ln(N-c)$, (a = 46.17 nm, b = 6.69 nm, c = 0.834))

The patterned chromium on fused silica was laser irradiated by different laser fluences Φ and number of laser pulses N. At high laser fluences already a single laser pulse induced a removal of the chromium and structuring of the fused silica surface. For Φ ≥ 1 J/cm², the resultant structure depth in fused silica increases almost linear with the laser fluence where the depth is independent on the number of laser pulses (see Fig. 1 (left), III). The depth – laser fluence can be described for 1 J/cm² ≤ Φ ≤ 2.3 J/cm² by a linear equation (see Fig. 1). Already a single pulse cause patterning of the fused silica in the fluence range for 610 mJ/cm² to 1 J/cm² but the pattern depth depends on the number of laser pulses (see Fig. 1 (left), III). The depth increased logarithmically with increasing number of laser pulses (see Fig. 1 (right)).
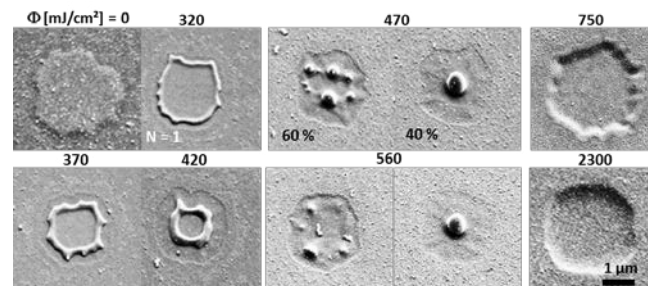

Fig. 2. SEM image of photolithographic structures ~7 nm chromium on fused silica irradiated by a single laser pulse with different laser fluences

The achievable structures in the fused silica are dependent on the laser parameters and on the original metal structure (see Fig. 2 and Fig. 3). At fluences Φ < 610 mJ/cm² the first laser pulse induces a modification of the shape of the chromium structure (see Fig. 2). For fluences from 320 mJ/cm² to 420 mJ/cm² the reduction of the lateral size of the chromium structures and the formation of a ridge can be found (see Fig. 2). In comparison to the original chromium covered area (coverage 100 %), single pulse irradiation with 420 mJ/cm² reduces the coverage to ~ 60 % (see Fig. 2 and 5). The formation of single and multiple droplet patterns occurs regularly for fluences between 470 mJ/cm² and 560 mJ/cm².

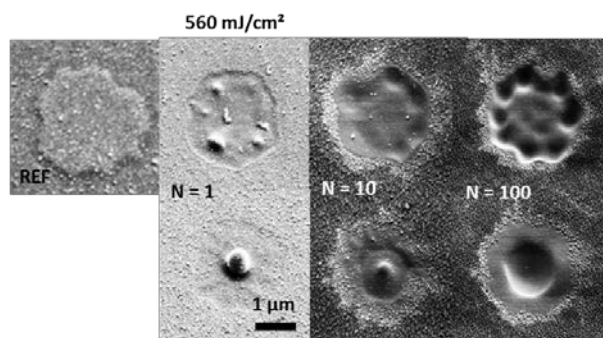Fig. 3. SEM images of laser-irradiated 7 nm chromium structure; two substantial different types of patterns are formed at Φ ~ 560 mJ/cm² and transferred into the fused silica at higher pulse numbers

Two different droplet distributions are observed: single droplets are formed with a probability of 40% in the centre of the original chromium structure as well as a multi-droplet formation at the border of the pattern is observed with a probability of 60%. Furthermore, multi-pulse irradiation of the chromium structure at ~ 560 mJ/cm² results in the structuring of the fused silica due to the transfer the metal pattern into the fused silica where the final structures shape is determined by the structures formed at the first pulse and morphology of the pattern depend on the number of laser pulses (see Fig. 3).

4. Theory

4.1. Heat equation

To improve the understanding of the laser-solid interaction the laser heating and phase transition of the chromium on a

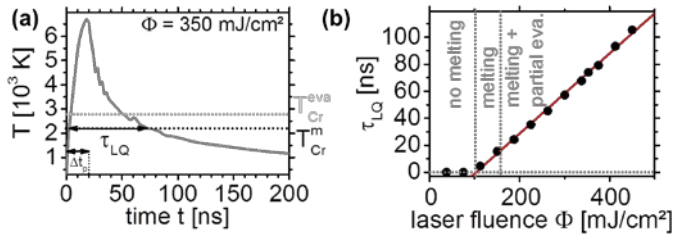fused silica substrate was calculated by solving the heat equation with a finite element method (FEM).

Fig. 4. (a) Calculated temperature dependent on time at the middle of the chromium at the Cr/SiO$_2$ interface at Φ = 350 mJ/cm³

(b) Estimated liquid phase life time based on the calculated beam profile

Therefore, the origin chromium structure was described by a cuboid with a lateral size of 2.5 x 2.5 μm² and a thickness of 7 nm. Further information of the used model is reported in [11]. An effective optical reflectivity R of 0.21 was assumed. Size-dependent absorption effects are neglected as the pattern size is much larger than the laser wavelength. The time-dependent temperature distribution (see Fig. 4 a) allows the estimation of the liquid phase lifetime τ_{LQ} (see Fig. 4 b) where the τ_{LQ} is dependent on the laser fluence Φ. The estimated τ_{LQ} can be analytically described by:

$$\tau_{LQ} = m \cdot (\Phi - \Phi_{th}) \tag{1}$$

with a slope of m = (0.297 ± 0.005) ns/(mJ/cm²) and laser fluence threshold Φ_{th} = (103 ± 6) mJ/cm² and a coefficient determination of R² = 0.997. Evaporation processes also neglected.

4.2. Navier Stokes equation

To simulate the mass transport, we used a special formulation of the Navier-Stokes equation as derived by Ghatak et al. [13].

In order to solve the equation, we used a finite differences discretization in space on a 40 × 40 grid. Time stepping was carried out using the BDF code IDA [14]. The calculation assumes a constant viscosity of the molten film. The simulation results dependent on the time are shown in Fig. 5. The required time t for pattern formation can be correlated to the liquid phase lifetime τ_{LQ} and thereby to the laser fluence (based on the Eq. 2). Furthermore, the mass transport in result in a modification of the metal morphology. The experimental and theoretical found droplet formation process can be described by the value of the surface coverage c of the chromium on fused silica substrate where the coverage of the initial state was set to 100 %. The theoretically estimated c dependent on t and Φ are summarized in Fig. 5 (ii).

5. Discussion

Laser irradiation of the photolithographic produced chromium patterns can results in different modification of the

chromium structure as well as in the structuring of the fused silica surface dependent on the laser parameter. At high laser fluence (Φ > 1 J/cm²), the laser irradiation causes in the complete ablation of the chromium and the partial evaporation of the adjacent fused silica.
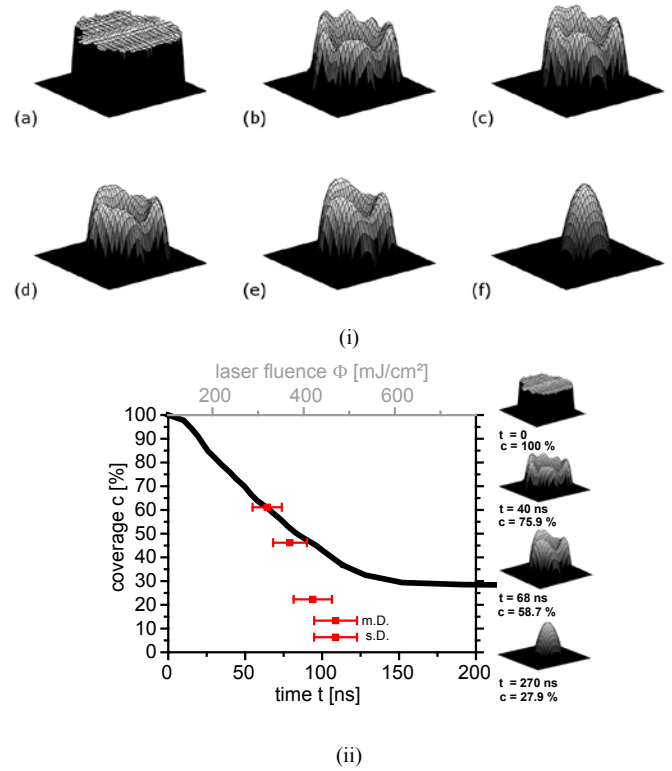

Fig. 5. (i) Simulation results (a) Initial configuration t =0 (z_{max} = 7 nm,), (b) after t = 40 ns (allocable laser fluence Φ based on Eq. 4: $\Phi \sim$ 240 mJ/cm², z_{max} = 14.7 nm) (c) t = 49.43 ns ($\Phi \sim$ 270 mJ/cm², z_{max} = 16.2 nm), (d) t = 57.58 ns ($\Phi \sim$ 300 mJ/cm², z_{max} = 17.5 nm), (e) t = 68 ns ($\Phi \sim$ 330 mJ/cm², z_{max} = 18.2 nm), (f) t = 270 ns final state ($\Phi \sim$ 1010 mJ/cm², z_{max} = 47.8 nm))

(ii) (black line) Estimated surface coverage c of the chromium on the fused silica surface based on the simulation (see Fig. 7 (i)) (initial configuration is set to c = 100 %) dependent on the time and the estimated laser fluence (based on Eq. 4); (red dot) experimental defined coverage based on the results (m.D. multi dot, s.D. single dot)

The depth of the fused silica structures increases linear with the laser fluence but does not rise with the pulse number (see Fig. 1). Similar results were found also for "classical" laser etching processes where the experimental result can be theoretical described by a thermodynamic model [2]. In this case, the thermodynamic model supposed an absorption of the laser energy by the metal layer and a following thermal diffusion into the dielectric surface. At sufficiently high laser fluences, a complete evaporation of the irradiated metal layer and a partial evaporation of the dielectric surfaces was simulated. That means, the simulation predicted a self-limiting structuring process and the structuring process stopped after the first laser pulse. Furthermore, the thermodynamic model predicted an almost linear depth-laser fluence behaviour in agreement with the found experimental results. Furthermore, the resultant structure is mainly defined by the initial lateral shape of the metal structure where a slight increase of the lateral shape of the transferred structures at increasing laser fluence can be found. A similar result was already reported at

[11]. At moderate laser fluence (~ 700 mJ/cm² < Φ < 1 J/cm²) the depth in the fused silica increases with the pulse number (see Fig. 1). This result is in disagreement with the thermodynamic model [2]. However, this effect can be most likely explained by the formation of modification layer near the surface of the fused silica that higher absorption allows the ablation for subsequent laser pulses [11]. The further multi-pulse irradiation of the formed additional modification layer results a partial evaporation of the modification layer and likely of the adjacent fused silica. The experimental results close the conclusion that, at suitable laser fluences (e.g. 750 mJ/cm², see Fig. 1 (right)), the formed modification layer can be found after various multi-pulses up to N = 1000 where the reduced ablation rate implied that the thickness and the composition is dependent on the number of laser pulses, respectively. The modification layer most likely consists of a chrome silicate [11]. The irradiation at low laser fluences (Φ < 700 mJ/cm²) results in melting and perhaps in partial evaporation of the chromium. The surface tension-driven mass transport in the liquid results finally in the formation of droplet patterns. At fluences from 470 to 560 mJ/cm², the irradiation result in the formation of a single or a multi-droplet formation (see Fig. 2). This result can be explained by the behaviour in the liquid metal film which is dependent on the characteristic length Λ of the molten instable film. The characteristic length is dependent on the surface tension γ ($\gamma \approx 1.7$ N/m), the Hamaker parameter A_H ($A_H \approx 5.7 \times 10^{-19}$ J) as well as film thickness h. It is given by:

$$\Lambda = \sqrt{\frac{16 \cdot \pi^3 \cdot \gamma}{A_H}} \cdot h^2 \qquad (2)$$

For a Cr film thickness of h = (6.9 ± 0.5) nm a characteristic length of Λ = (1.84 ± 0.27) μm was estimated. If the used size of the metal structures is smaller than Λ the formation of single metal droplets in the centre of the lithographically defined Cr patterns are probably. For larger metal structure randomly distributed patterns consisting of metal droplets with different size can be expected. In the experimental analyzed case, the pattern size is almost similar to Λ. This explains the experimental results. Furthermore, the process was approximated by a combination of heat equation (laser-solid interaction inclusive phase transition) and Navier-Stokes equation (mass transport in liquid) [12]. In this study, however, both differential equations are solved in sequence, see [12], but the simulation results represent well the experimental results [12]. In particular, the liquid phase lifetime that depends on the laser fluence was calculated by the heat equation and feed into the solving process of the Navier-Stokes equation. The calculated mass transport patterns in the liquid film are frozen at the end of the liquid phase lifetime. The experimentally found shape of the metal structures can be described very well by the simulations (see Fig. 2 and 5) for very low laser fluence (Φ ≤ 420 mJ/cm²). The differences between the experimental and the simulation results for higher fluences can be explained by partial evaporation of the chromium that is not considered in the simulations. In particular, the experimentally found smaller features can be discussed by the material loss for higher

fluences (see Fig 5 (ii)). Hence, simultaneous solving of both the heat and the Navier Stokes equation will be necessary to improve the simulation results. The further irradiation of the modified chromium structures with e.g. ~ 560 mJ/cm² results in an evaporation of the chromium and of the fused silica in parts where the resultant fused silica structure are dependent lateral shape of the laser-structured metal film (see Fig. 3). The SEM image suggests the conclusion that the structuring process is assisted by a formation of a modification layer.

6. Conclusion and Outlook

The laser-irradiation of photolithographic fabricated chromium structures results in the formation of determined and randomly distributed chromium structure. The lateral geometry of the formed metal structures can be transferred into the dielectric surface. The modification of the shape of the metal structures can be described well by a combination of a heat and a Navier Stokes equation where the simulation needs improvement for higher fluences by the considering evaporation process. The presented concept open the ways for the cost-effective fabrication of sub-μm and nanostructures based on microstructures produced by UV lithography.

Acknowledgements

References

[1] Ehrhardt, M., Lorenz, P., Zimmer, K., Surface modification by laser etching using a surface-adsorbed layerThin Solid Films 2012, 520: 3629–3633.

[2] Lorenz, P., Ehrhardt, M., Zimmer, K., Laser-induced front side and back side etching of fused silica with KrF and XeF excimer lasers using metallic absorber layers: A comparison, Appl. Surf. Sci.2012, 258: 9742–9746.

[3] Böhme, R., Zimmer, K., Ruthe, D., Rauschenbach, B., Backside Etching at the Interface to Diluted Medium with Nanometer Etch Rates, J. Laser Micro/Nanoeng. 2006, 1: 190–194.

[4] Konstantaki, M., Childs, P., Sozzi, M., Pissadakis, S., Relief Bragg reflectors inscribed on the capillary walls of solid-core photonic crystal fibers, LaserPhotonics Rev. 2013, 7: 439–443.

[5] Ehrhardt, M., Raciukaitis, G., Gecys, P., Zimmer, K., Laser-induced backside wet etching of fluoride and sapphire usingpicosecond laser pulses, Appl. Phys. A 2010, 101: 399–404.

[6] Lorenz, P., Ehrhardt, M., Zimmer, K., Laser-Induced front Side Etching: An Easy and Fast Method for Sub-μm Structuring of Dielectrics Physics Procedia 2012, 39: 542–547.

[7] Lorenz, P., Frost, F., Ehrhardt, M., Zimmer, K., Laser-induced fabrication of randomly distributed nanostructures in fused silica surfaces. Appl. Phys. A 2013, 111: 1025-1030.

[8] Lorenz, P., Zajadacz, J., Bayer, L., Ehrhardt, M., Zimmer, K., Nanodrilling of fused silica using nanosecond laser radiation, Appl. Surf. Sci. 2015, 351: 935–945.

[9] Lorenz, P., Zagoranskiy, I., Ehrhardt, M., Bayer, L., Zimmer, K., Nanostructuring of sapphire using time-modulated nanosecond laser pulses, Proc. SPIE 10092, Laser-based Micro- and Nanoprocessing XI, 100921P (February 17, 2017); doi:10.1117/12.2251826.

[10] Lorenz, P., Zajadazc, J., Ehrhardt, M., Bayer, L., Zimmer, K., Pattern transfer, self-organized surface nanostructuring, and nanodrilling of sapphire using nanosecond laser irradiation, Proc. SPIE 9736, Laser-based Micro- and Nanoprocessing X, 97361K (March 4, 2016); doi:10.1117/12.2212122.

[11] Lorenz, P., Grüner, C., Ehrhardt, M., Bayer, L., Zimmer, K., Nanostructuring of fused silica assisted by laser-shaped metal triangles using a nanosecond laser, Physics Procedia 2016, 83: 62-73.

[12] Lorenz, P., Klöppel, M., Smausz, T., Csizmadia, T., Ehrhardt, M., Zimmer, K., Hopp, B., Dynamics of the laser-induced nanostructuring of thin metal layers: experiment and theory, Mater. Res. Express 2015, 2: 026501.

[13] Ghatak, A., Khanna, R., Sharma, A., Dynamics and Morphology of Holes in Dewetting of Thin Films, J. Coll. Inter. Sci 1999, 212: 483–494.

[14] Hindmarsh, A. C., Brown, P. N., Grant, K. E., Lee, S. L., Serban, R., D. E. Shumaker, D. E., Woodward, C. S., SUNDIALS: Suite of nonlinear and differential/algebraic equation solvers, ACM TOMS 2005, 31-3(2005) 36.